Revision date: 7 August 2025

Layering in tailings deposits: Characterization and implications for CPT interpretation

A.T. Owolabi, *MSc*; L.A. Torres-Cruz, *PhD, MICE, CEng*

First author:

- PhD student at the School of Civil and Environmental Engineering of the University of the Witwatersrand, Johannesburg, South Africa.
- 1250863@students.wits.ac.za

Second author:

- Assistant Professor at the Norman B. Keevil Institute of Mining Engineering at the University of British Columbia, Vancouver, Canada
- Visiting lecturer at the University of the Witwatersrand, Johannesburg, South Africa.
- ORCID number: 0000-0001-8482-0070
- Luis.TorresCruz@ubc.ca

Abstract

The cone penetration test (CPT) is widely used for tailings characterisation. Often, the CPT is used to infer the state parameter (ψ) using methods based on uniform soil specimens. This paper addresses a crucial question: To what extent do tailings deposits resemble uniform specimens? We quantitatively characterised layering in tube samples from three active gold tailings storage facilities (TSFs) and visually appraised a 3 m profile at a fourth TSF. Results reveal pronounced thin layering in all samples and the exposed profile. Our analysis suggests that the uniform layers documented herein are unlikely to exceed 10 cm. This is significantly less than the >0.6 m recommended for CPT interpretation. The PSD variability within a single 25 cm sample often matched or exceeded that observed across entire TSFs, highlighting the significance of the variability. Thin layering constitutes a significant deviation from the uniformity assumption underpinning widely used CPT interpretation methods and is likely to compromise the accuracy of CPT-based ψ estimates. Thin layering also raises fundamental questions about validating ψ estimates. We propose shifting research to include the approximate laboratory characterisation of layered specimens rather than focusing on the precise characterisation of uniform specimens that do not resemble in situ conditions.

List of notations

λ	Slope of the CSL in e-$\log_{10}p'$ space
ψ	State parameter
CC	Calibration chamber
CPT	Cone penetration test

CSL	Critical state line
CSSM	Critical state soil mechanics
D_n	Particle size that corresponds to n% of the PSD curve
DP	Tailings discharge point
e	Void ratio
G_s	Specific gravity of the particles
M_{tc}	Critical state friction ratio measured in triaxial compression
OvFl	Overflow from hydrocyclone
p'	Mean effective stress
PL	Plastic limit
PSD	Particle size distribution
SEM	Scanning electron microscopy
TSF	Tailings storage facility
UnFl	Underflow from hydrocyclone
X_{tc}	Stress-dilatancy property measured in triaxial compression

Keywords

Tailings, CPT interpretation, layering, CSSM

1 Introduction

The cone penetration test (CPT) is likely the most widely used in situ geotechnical test to characterize tailings (Ayala et al., 2022; Fourie et al., 2022). Several CPT interpretation methods

aim at inferring the state parameter (ψ) which is the void ratio (e) difference between a soil and its critical state line (CSL) at the current mean effective stress (p') (Been & Jefferies, 1985). The state parameter ψ is indicative of a soil's volume change tendencies at large strains and therefore of several aspects of engineering behaviour. The first efforts to infer ψ from the CPT were based on data from calibration chamber (CC) testing supplemented by soil properties measured through triaxial testing (Been et al. 1986; 1987). CCs have a height and diameter of ~1 m and essentially allow a full-scale CPT to be performed in a laboratory environment in which soil characteristics, density, and stress levels can be controlled or measured.

CC tests and the supplementary laboratory testing use soil specimens that are as uniform as possible in terms of ψ as this is necessary to develop correlations with cone tip resistance. This translates to CC specimens with a uniform e and a constant particle size distribution (PSD), particle shape, and mineralogy to ensure a unique CSL. Techniques such as dry pluviation through sieves (Huntsman, 1985) or moist tamping after homogenization (Been et al., 1987) have been used to achieve the desired CC specimen uniformity. Similar approaches are used to achieve uniform triaxial specimens (Ayala et al., 2022; Been & Olivera, 2016; da Fonseca et al., 2021).

The framework proposed by Been et al. (1986; 1987) has been modified and expanded by numerous authors. Numerical simulations of cavity expansion, used as a CPT proxy, imply that the framework can be implemented without having to perform CC tests (Shuttle & Jefferies, 1998). However, the newer methods retain the link to CC results and the dependency on soil properties measured in the laboratory e.g. (Shuttle & Cunning, 2007; Shuttle & Jefferies, 2016;

Jefferies et al., 2019; Shuttle et al., 2022; Mozaffari & Ghafghazi, 2024) or estimated from CPT readings e.g. (Plewes et al., 1992; Jung et al., 2025).

The widespread use in tailings engineering of CPT interpretation methods that are based on the Been et al. (1986; 1987) framework is reflected in the investigations of some of the most prominent tailings storage facility (TSF) failures. For example, the investigations of TSF failures such as Samarco (Morgenstern et al., 2016), Cadia Valley (Jefferies et al., 2019), and Brumadinho (Robertson et al., 2019; CIMNE, 2021), collectively used the CPT interpretation methods described in Plewes et al. (1992), Shuttle and Cunning (2007), and Shuttle and Jefferies (2016). The heavy reliance on this family of methods prompts the question of the extent to which tailings deposits resemble the uniform CC and triaxial specimens that underpin the methods. Layered deposits complicate CPT interpretation for at least two reasons. Firstly, they constitute an important deviation from the conditions used to develop the Been et al. (1986; 1987) framework. And secondly, in layered deposits multiple soils simultaneously affect cone response (Boulanger & DeJong, 2018; Tehrani et al., 2017). Therefore, if a CPT interpretation method requires soil properties, it is not clear which of the layered soils should be tested in the laboratory. No studies, to the authors' knowledge, have validated the use of homogenized sample properties for CPT interpretation in layered tailings. Accordingly, it has been recommended that, to avoid interference from adjacent layers, CPT interpretation should focus on layers that are >0.6 m thick and have a stiffness ratio <5 between adjacent materials (Jefferies & Been, 2016). For instance, Shuttle and Cunning (2007) reported CPT-based ψ estimates in a silt layer that was ~8 m thick and which exhibited approximately constant values of a soil behaviour type index

derived from CPT readings. A unique set of soil properties was assigned to this layer, implying that it was believed to be uniform.

Multiple works have incidentally or qualitatively reported tailings layering (Blight, 2010; da Fonseca et al., 2020; Jacobsz & Narainsamy, 2022; Vick, 1990). However, there is limited literature focusing on quantitative characterisation of such layering. For instance, Vermeulen (2001) reported vertical profiles at a gold TSF that, based on colour changes, exhibited layers that in some cases were only a few centimetres thick. Reid et al. (2018a) reported gradation results of subaqueously deposited iron ore tailings and, based on the percentage passing the 38 and 75 µm sieves, found negligible signs of layering. Reid and Fanni (2022) reported results from two block samples of iron ore tailings from which they extracted PSD specimens at ~2 cm intervals. Based on the percentages passing the 38 µm sieve, they reported modest PSD variations. However, it is inferred from Reid and Fanni (2022) that they made an effort to sample blocks that did not exhibit layering to enable comparisons between intact and reconstituted samples. Reid et al. (2022) examined block samples of gold, platinum and copper tailings. By considering the percentages passing the 38 and 75 µm sieves, they concluded that the blocks were layered and exhibited a wide range of gradations.

The reviewed literature suggests that while thick uniform tailings layers may exist in some TSFs, thinly layered structures can also develop. However, it is not clear how prevalent such layering is. Furthermore, investigations into tailings layering have described PSD curves with only one or two points. The importance of layering on CPT interpretation suggests that more detailed PSD descriptions are warranted. The authors were also unable to find any works that explicitly discuss

the implications of tailings layering on CPT interpretation. Herein, we characterise the layering in high-quality samples, sometimes referred to as undisturbed samples, from three active South African TSFs with varied hydraulic deposition methods. Additionally, we appraise a 3 m deep vertical profile at a TSF undergoing reclamation. We discuss the implications of our results on CPT interpretation.

2 Methodology

2.1 Sites investigated

The fieldwork focused on gold tailings from the Witwatersrand Basin near Johannesburg, South Africa. Four upstream TSFs were investigated. Surface high-quality samples that preserved the in situ layering were taken from three active TSFs, while visual inspections were performed at the fourth TSF. To account for different deposition methods, the three sampled TSFs were chosen to represent different depositional methods: cycloning, paddocking, and spigotting. Cycloning uses hydrocyclones to separate the tailings feed into a coarse fraction (underflow) and a fine fraction (overflow) deposited on the outer and internal part of the TSF, respectively. Paddocking involves depositing tailings in enclosed areas (the paddocks) on the outer wall of the dam during the day and depositing in the internal part of the TSF at night. Spigotting uses outlets or spigots connected to a main delivery pipe that runs along the perimeter of the outer wall of the TSF. Detailed descriptions of these methods have been previously reported (Blight, 2010; McPhail & Wagner, 1987). Hereafter, the three sampled TSFs will be referred to simply as the Cyclone TSF, Paddock TSF, and Spigot TSF. The fourth investigated TSF was undergoing tailings reprocessing and this allowed inspection of layering patterns along profiles that were several metres long. This

TSF also adopted paddocking deposition and will be referred to as the Remine TSF. Figure 1 shows the locations of the TSFs and Figure 2 shows their overall layout.

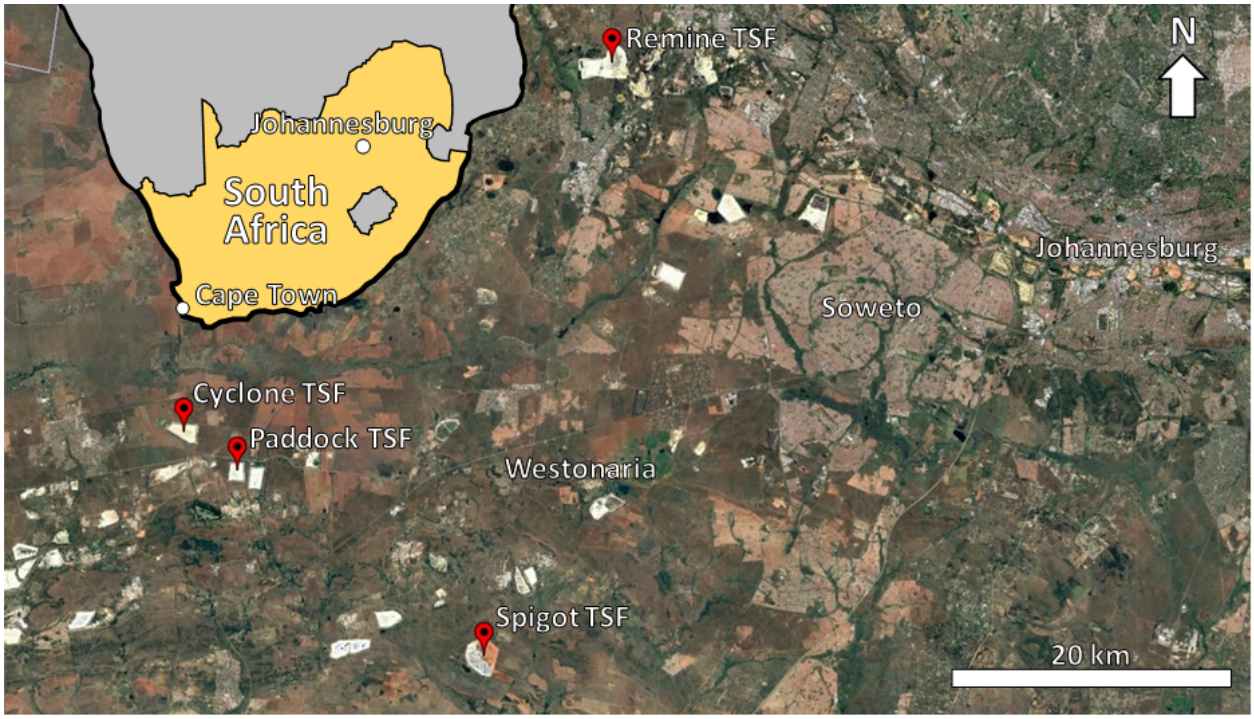

Figure 1. Location of the Cyclone, Paddock, Spigot, and Remine TSFs with respect to Johannesburg, South Africa. (Source: Google Earth Pro).

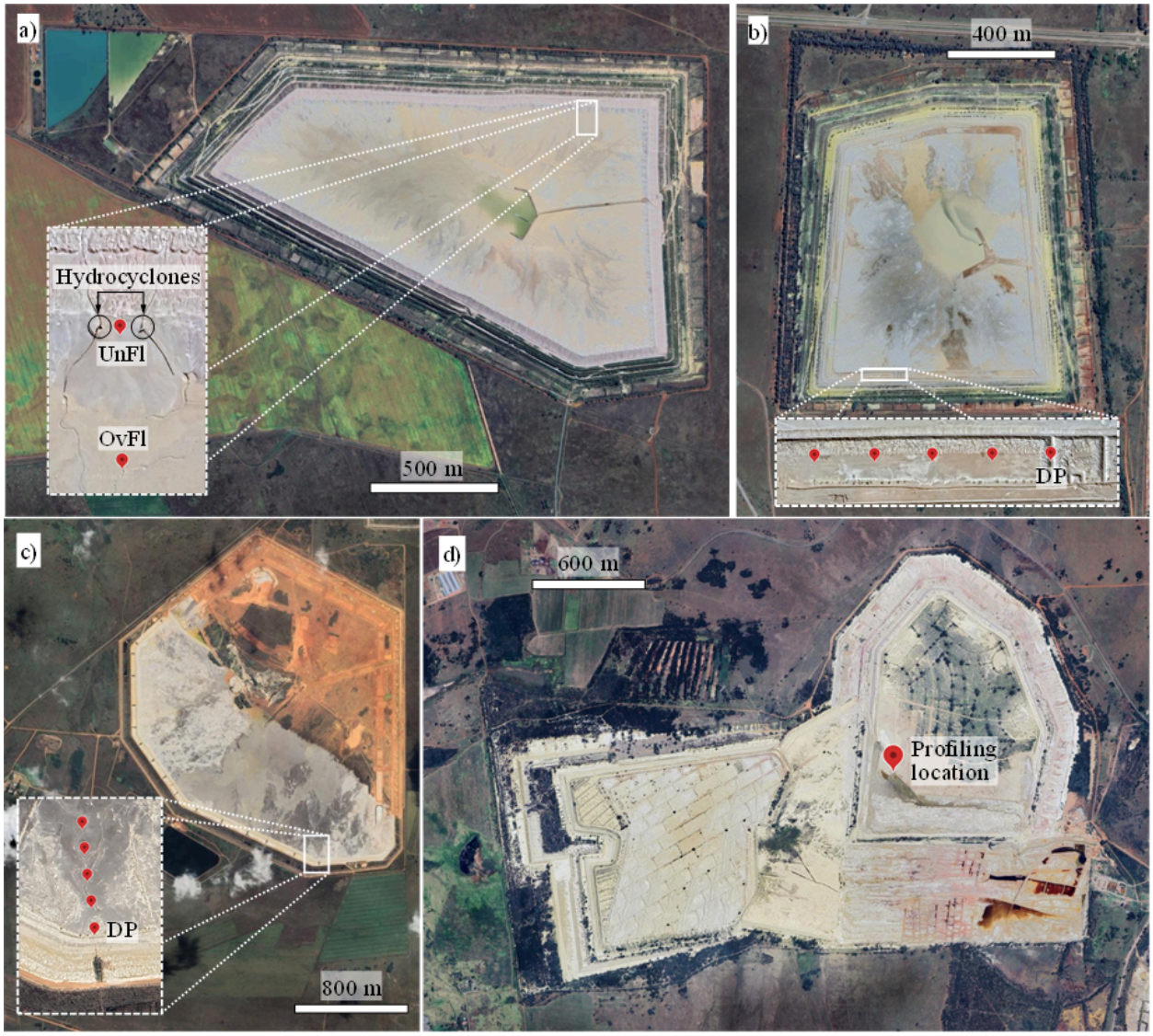

Figure 2. Satellite images of the investigated TSFs: a) Cyclone TSF; b) Paddock TSF; c) Spigot TSF; and d) Remine TSF. Notes: Insets in parts a) to c) show sampling locations. OvFl = overflow; UnFl = underflow, DP = Discharge point (not sampled). Source: Google Earth Pro.

2.2 Sampling and characterization of tailings

A stainless-steel split tube sampler (Figure 3) was manufactured to extract shallow samples that preserved any potential layering. The sampler meets the requirements of ASTM D1587-15

158 (ASTM, 2015) and is similar to a sampler previously used for gold tailings (Vermeulen, 2001).
159 The upper portion of the sampler consists of a split solid cylinder that has a 1 mm diameter vent
160 hole through its centre. The hole also enabled the insertion of a 0.75 mm rod used to check that
161 the sampler was full. The sampling tube is 250 mm long with inner and outer diameters of 75
162 and 80 mm. The lowest 25 mm of the sampling tube are tapered at 5° to facilitate sampling. The
163 tube was polished inside and out to minimise friction.
164

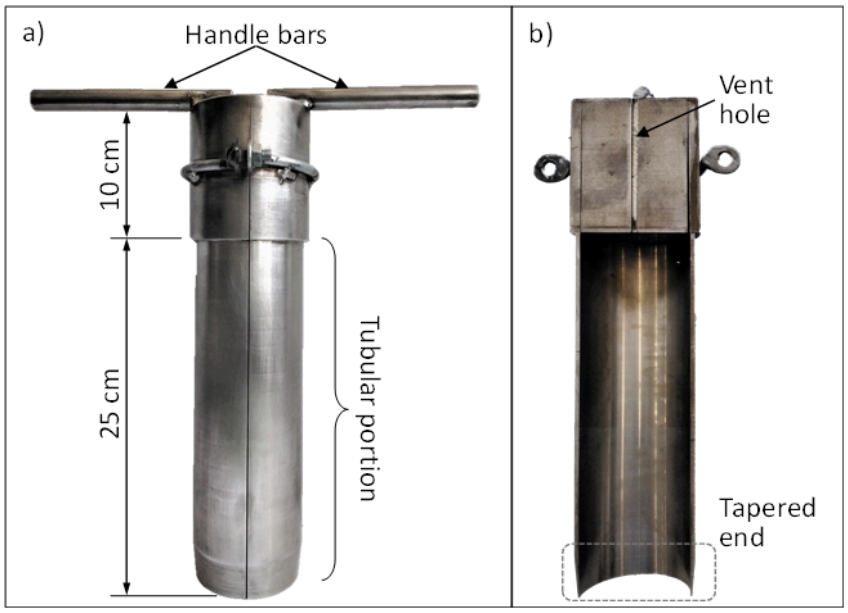

165

166 **Figure 3.** Tailings sampler: a) assembled and b) internal lateral view of one half.

167

168 During sampling, the entire length of the sampling tube was pushed into the tailings from surface
169 level. To minimise disturbance, the sampler was then dug out rather than pulled out.
170 Subsequently, the sampler was opened and the sample marked at 1 cm intervals to obtain 25
171 slices (Figure 4). A cutting plate was then used to slice the sample and each slice was stored in a
172 labelled, air-tight bag for transportation to the laboratory. For each sample, the slices were
173 numbered from 1 to 25 from top to bottom. To achieve a uniform slicing frequency, the slices

were always cut at 1 cm intervals regardless of the layer boundaries suggested by colour changes. However, assuming that colour changes reflect alterations in PSD and mineralogy, some layers could have been thinner than 1 cm (e.g. the lowest three centimetres of the sample in Figure 4).

Ten samples, resulting in 250 slices, were collected from the locations shown in Figure 2. At the Cyclone TSF, both the underflow and the overflow were sampled. And for the Paddock and Spigot TSFs samples were collected at different distances from the discharge point. Table 1 provides additional details regarding the sampling locations and the code used to identify each sample. The code is composed of the name of the TSF and an indication of the distance from the discharge point or, in the case of the Cyclone TSF, of whether the sample was of the underflow or overflow. Individual slices will be identified herein by adding the slice number to the code of the sample. For example, slice *Cyclone UnFl (7)* is the seventh slice from top to bottom of the underflow sample at the Cyclone TSF.

Figure 4. Sample Spigot @100 with marks at 1 cm intervals prior to being sliced.

Table 1. Location and code of the ten samples recovered with the tube sampler.

TSF	Location	Code
Cyclone	9 m along outer wall from underflow discharge (Figure 2a).	Cyclone UnFl
	35 m towards the decant pond from overflow discharge (Figure 2a).	Cyclone OvFl
Paddock	25, 50, 75, and 100 m from discharge within the paddock (Figure 2b).	Paddock @25 Paddock @50 Paddock @75 Paddock @100
Spigot	25, 50, 75, and 100 m from discharge towards the decant pond (Figure 2c).	Spigot @25 Spigot @50 Spigot @75 Spigot @100

The particle shape of the tailings from the three sampled TSFs was examined using scanning electron microscopy (SEM) on three tailings size fractions isolated by sieving (>150 µm, 75 to 150 µm, and <75 µm). The particles were highly angular regardless of particle size (Figure 5), which is characteristic of tailings generated from ore crushing e.g. (Torres-Cruz & Santamarina, 2020; Vermeulen, 2001).

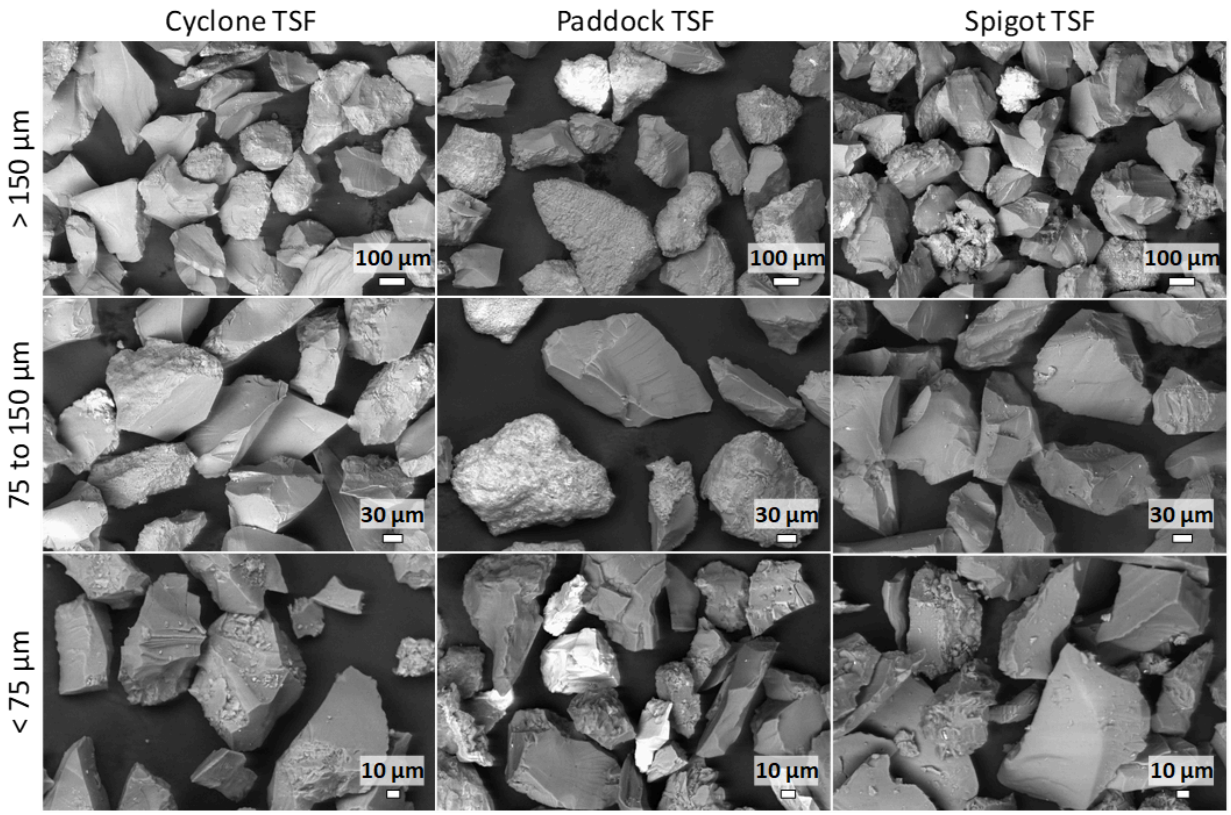

Figure 5. Scanning electron microscopy images of the sampled tailings.

The mineralogy of one slice from each sampled TSF was analysed using X-ray diffraction. The analysed slices exhibited a PSD that was deemed representative of the respective TSF. Table 2 summarises the mineralogy and shows that the tailings from all three TSFs are dominated (>55%) by quartz. This agrees with previous reports of the mineralogy of gold tailings from the Witwatersrand Basin (Chang, 2009; Vermeulen, 2001). The tailings also contained significant amounts (> 8%) of chlorite. Additionally, the Paddock TSF exhibits significant amounts (> 8%) of plagioclase, muscovite, and actinolite.

211 **Table 2.** Mineralogy of three sampled TSFs.

212

Mineral	Cyclone OvFl (2)	Paddock @25 (17)	Spigot @100 (8)
Quartz	77.5	56.4	74.6
Plagioclase	0	8.9	0
Chlorite	8.4	8.5	8.6
Microcline	0	1.6	0
Muscovite	4.6	8.1	3.2
Pyrophyllite	2.9	4.5	5.8
Talc	0	0	5.3
Hematite	0.6	0	0
Chloritoid	4.0	0	0
Pyrite	0	0	0.7
Dolomite	0	2.9	0
Gypsum	2.0	0	0
Actinolite	0	9.1	0
Calcite	0	0	1.8

213

214 The specific gravity (G_s) was measured following BS 1377:2 (BSI, 1990) for the finest and
215 coarsest slice encountered at each TSF. For the Cyclone TSF and the Paddock TSF the G_s was
216 2.70 and 2.72, respectively, for both slices. For the Spigot TSF the fine slice yielded 2.59 and the
217 coarsest 2.67. These results are consistent with the quartz-dominated mineralogy (Table 2) and
218 previous G_s values reported for gold tailings (Chang, 2009; Vermeulen, 2001).

219

In order to assess variability along the length of the samples, the PSD and plastic limit (PL) of each slice were determined. PSD determinations were done in a laser diffraction spectroscopy device (Anton Paar PSA 1090) which operates on particle sizes ranging from 0.04 to 500 μm. The specimen mass required for the PSD determinations ranged between 0.9 and 1.4 g. Each PSD specimen was extracted from the central portion of the top surface of each slice. The dispersing agent was sodium hexametaphosphate (5 g/litre) as per ASTM D7928-21 (ASTM, 2021). The specimens and the dispersing solution were placed in a covered container and left overnight in the temperature-controlled room that housed the laser diffraction device to ensure temperature equilibrium and promote deflocculation. PL determinations followed the thread rolling method of BSI 1377:2 (BSI, 1990). Additional index properties, such as the liquid limit or the minimum and maximum void ratio were not determined due to the limited mass of each slice.

2.3 Profiling at the Remine TSF

The reclamation activities at the Remine TSF allowed us to expose a 3 m deep profile for visual appraisal at the location shown in Figure 2d. To this end, we adopted an approach similar to that described in Vermeulen (2001). Six 0.5 m tall benches were created by cutting into the tailings with the flat blade of a spade. The vertical faces were then individually photographed.

3 Results

3.1 Layering characteristics in the sampled tailings

Figures 6 to 8 show the 25 PSDs measured on each sample collected at the Cyclone, Paddock, and Spigot TSFs. At the Cyclone TSF, the range of gradations is broader for the underflow

sample than for the overflow sample (Figure 6). At the Paddock TSF, the samples collected 25 and 50 m away from the discharge point exhibited the broadest range of gradations. Whereas the samples collected 75 and 100 m away from the discharge point exhibited narrower and finer gradations. This is consistent with the general trend of coarser particles settling out of the slurry closer to the discharge point (Blight, 2010). As for the Spigot TSF, the sample collected at 100 m from the discharge point exhibited the broadest range of gradations. The four Spigot TSF samples do not reveal a clear trend of PSDs getting finer as the distance from the discharge point increases. This is not entirely surprising, as data from Blight (2010) suggests that in some cases it is necessary to collect samples over longer distances along the beach for clear PSD trends to emerge.

To contextualise our results Figures 6 to 8 include the PSD envelopes of two TSFs that failed in Brazil: The Samarco TSF (Rezende, 2013) and the Córrego do Feijão TSF (Robertson et al., 2019). The Samarco TSF failure is sometimes referred to by the name of the failed containment structure which was the Fundão Dam. And the Córrego do Feijão TSF failure is better known by the name of the nearby town, Brumadinho. The PSD envelope for Fundão is based on 26 samples of which 18 correspond to the tailings slurry as it leaves the concentration plant, and 8 correspond to samples taken over a 110 m distance that stretched from the dam crest into the tailings beach (Rezende, 2013). The PSD range for the Brumadinho TSF is based on 20 samples described as coarse, fine, or berm fill tailings in Robertson et al. (2019). The samples from both TSFs aimed at characterizing the different types of impounded tailings.

The PSD envelopes of the Fundão and Brumadinho PSDs are generally coarser than the PSDs measured in our ten samples. Accordingly, to facilitate comparison, the reference envelopes were shifted to the left by dividing all the particle sizes of the envelopes by a number which varies across plots and is indicated in the legends of Figures 6 to 8. Because the horizontal axis is logarithmic, this division does not alter the shape of the envelopes.

Figures 6 to 8 show that the range of PSDs in a single 25 cm sample is often comparable, and sometimes even larger, than the PSD envelopes inferred from samples collected from different parts of a TSF. This is particularly true when comparing the sample PSDs to the Fundão PSD envelopes which are narrower than those at Brumadinho. However, even the wider range of the Brumadinho PSDs is similar to the PSD variability of some samples (Figure 7a, b and Figure 8d). It seems likely that if the PSD samples at Brumadinho and Fundão had been subjected to the detailed slicing adopted herein, their PSD envelopes would have been wider. Notwithstanding, Figures 6 to 8 suggest that the PSD variability that occurs along a small 25 cm sample is not merely a minor deviation from a central trend, but rather a variability that is comparable to that observed across an entire TSF.

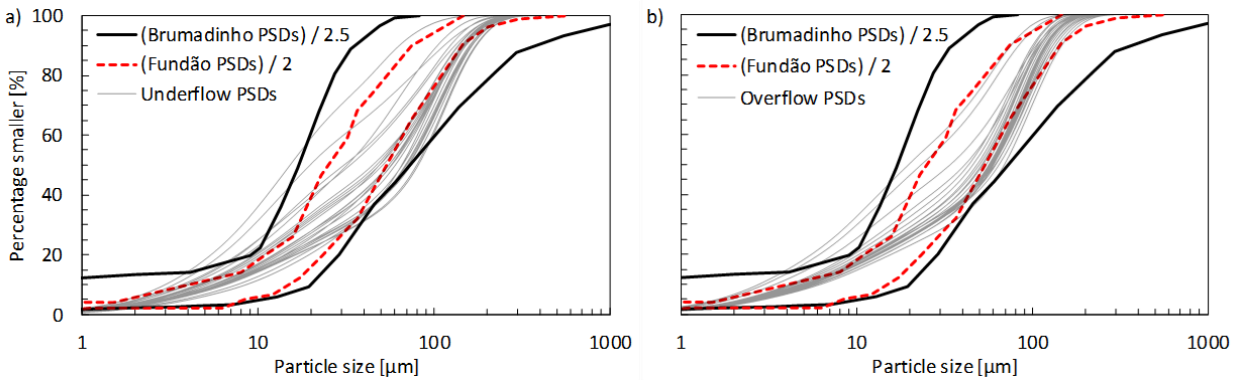

279

280 **Figure 6.** Range of PSDs in the samples a) Cyclone UnFl and b) Cyclone OvFl. Note: Laterally
281 shifted PSD envelopes shown for Fundão (Rezende, 2013) and Brumadinho (Robertson et al.,
282 2019).

283

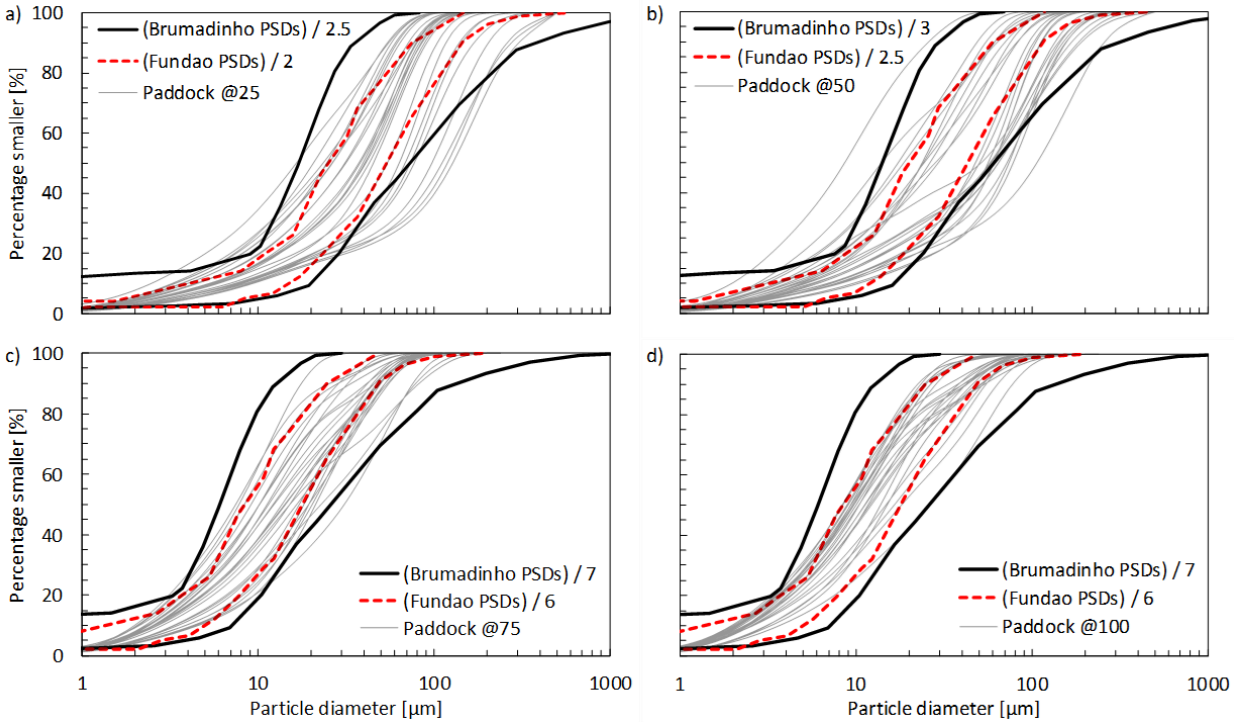

284

285 **Figure 7.** Range of PSDs in the samples a) Paddock @25, b) Paddock @50, c) Paddock @75,
286 and d) Paddock @100. Note: Laterally shifted PSD envelopes shown for Fundão (Rezende,
287 2013) and Brumadinho (Robertson et al., 2019).

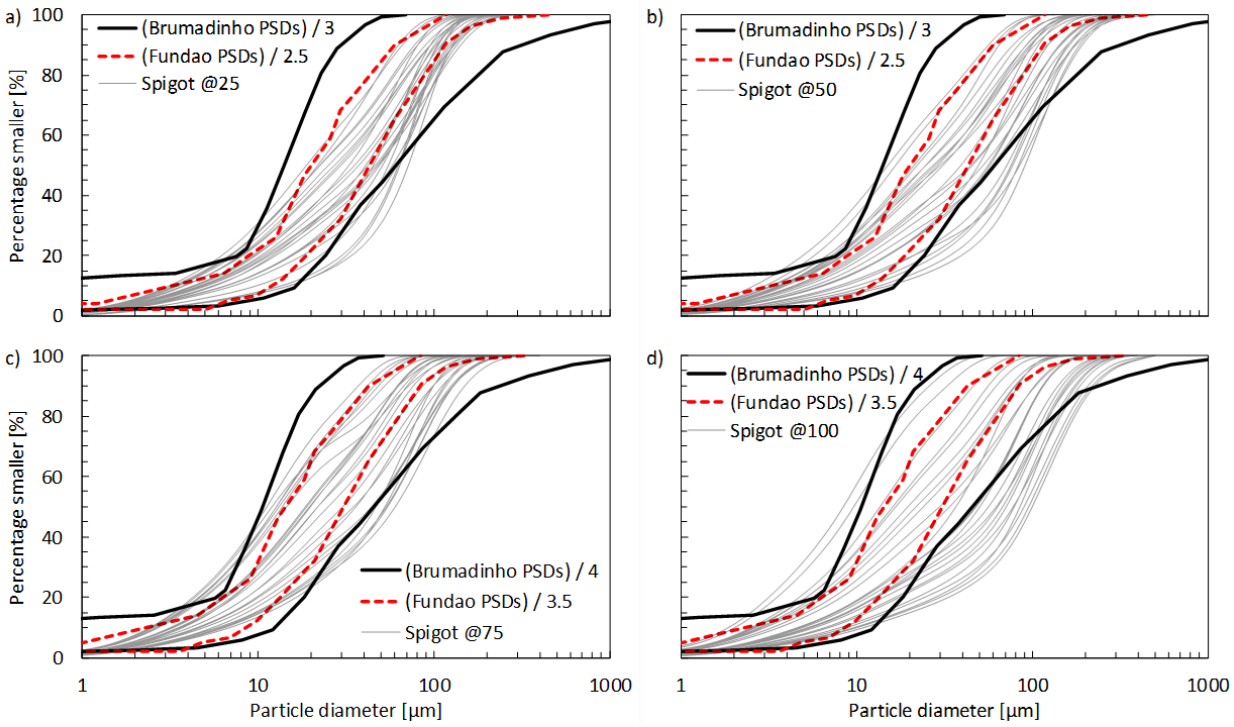

Figure 8. Range of PSDs in the samples a) Spigot @25, b) Spigot @50, c) Spigot @75, and d) Spigot @100. Note: Laterally shifted PSD envelopes shown for Fundão (Rezende, 2013) and Brumadinho (Robertson et al., 2019).

Figure 9 shows profiles of D_{10}, D_{50}, and D_{90} along the height of the ten samples. The plots further highlight how changes in gradation occur over centimetres. The profiles suggest that the thickest uniform layer in all ten samples corresponds to the upper ~15 cm of the Cyclone OvFl sample (Figure 9b). This is consistent with the narrower band of PSDs observed in Figure 6b.

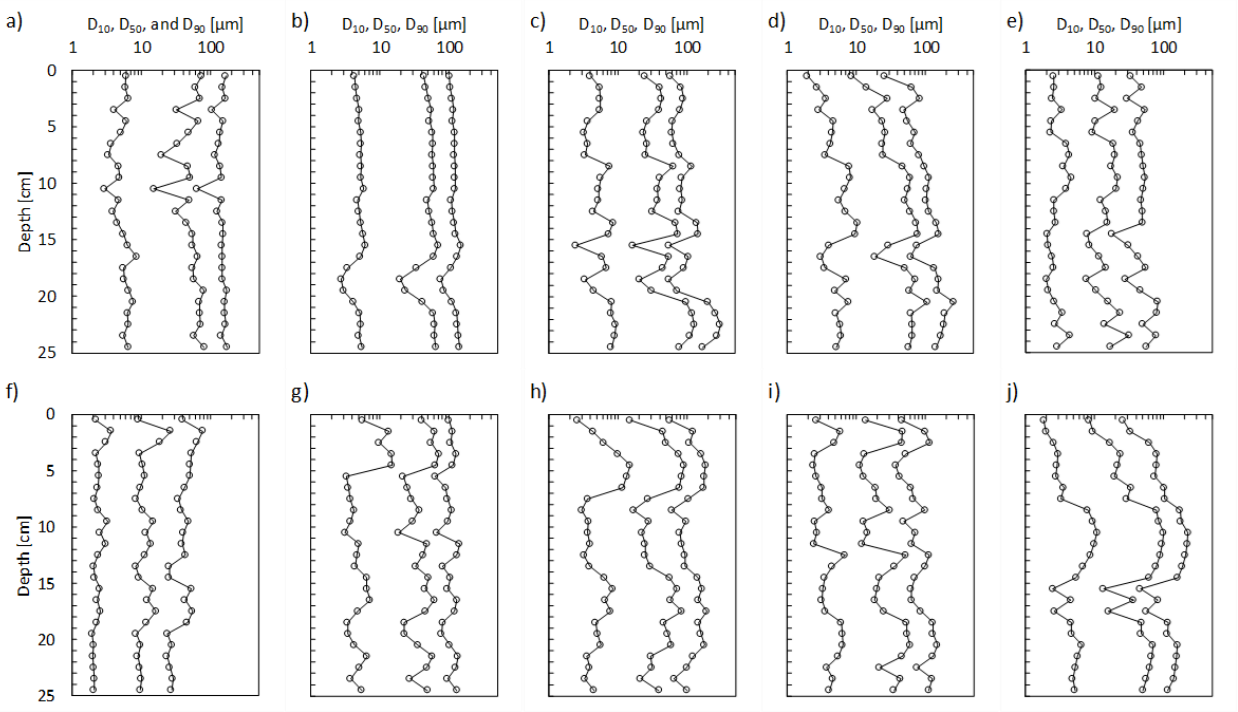

299

300 **Figure 9.** Profiles of D_{10}, D_{50}, and D_{90} of samples a) Cyclone UnFl, b) Cyclone OvFl, c) Paddock
301 @25, d) Paddock @50, e) Paddock @75, f) Paddock @100, g) Spigot @25, h) Spigot @50, i)
302 Spigot @75, and j) Spigot @100.

303

304 Plastic limits (PL) could not be measured for the large majority of the slices because the
305 nonplastic nature of the tailings prevented them from being rolled into threads. Table 3
306 summarises the limited PL results obtained. All values fall within a relatively low and narrow
307 range of 23 and 33%. This suggests that while PSD varied significantly within the samples,
308 plasticity did not.

309

Table 3. Plastic limit results.

TSF	Sample	Slice numbers	PL Range (%)
Paddock	Paddock @ 50m	1 – 2	23 – 27
	Paddock @ 75m	2 – 4 and 13 – 20	24 – 32
	Paddock @ 100m	3 – 15	24 – 33
Spigot	Spigot @ 75m	5 – 7	27 – 32
	Spigot @ 100m	1 – 2	30 – 33

3.2 Layering in the exposed profile of the Remine TSF

Figure 10 shows photographs of the 3 m profile exposed at the Remine TSF. Assuming that changes in colour reflect changes in mineralogy or PSD, the thinly layered nature of the tailings deposit is evident. Several portions exhibit layers that are only a few millimetres thick (e.g., between 20 and 40 cm, 130 and 140 cm, and 170 and 180 cm). Overall, the figure suggests that uniform layers at the Remine TSF are unlikely to exceed thicknesses of 10 cm.

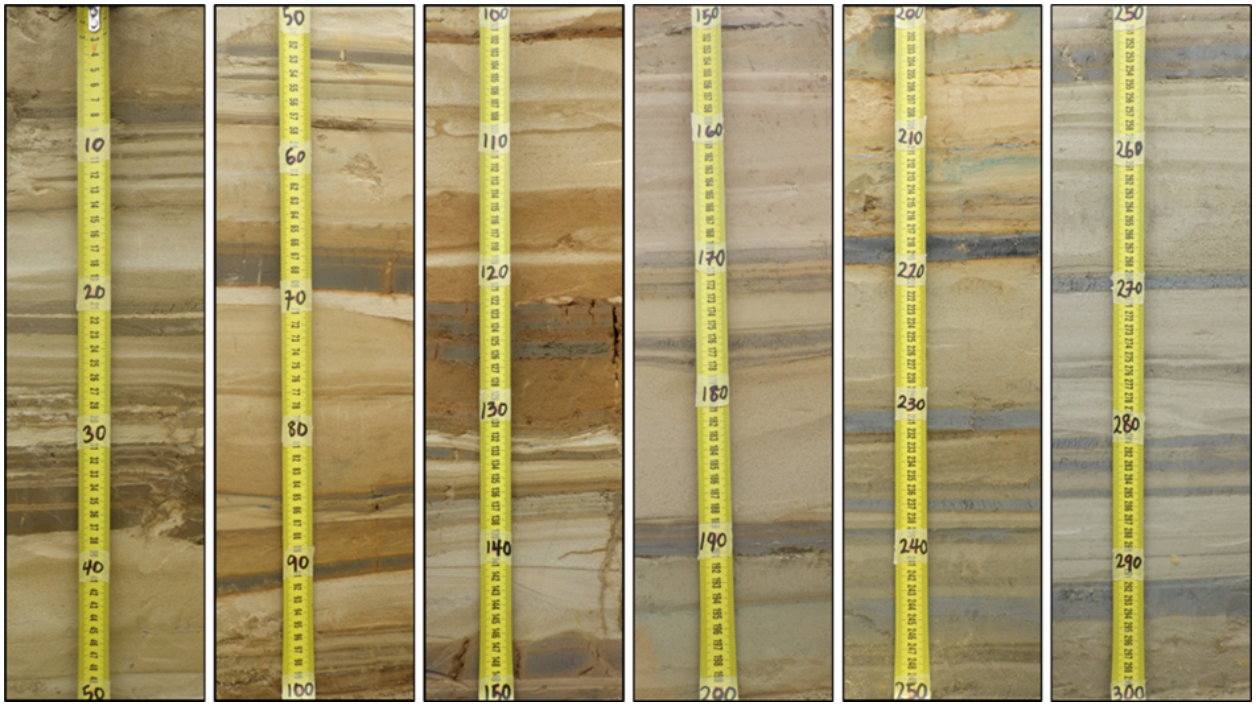

Figure 10. Photographs of the 3 m deep profile at the Remine TSF. Note: Measuring tape shows centimetres.

4 Discussion

PSD analyses of ten 25 cm tube samples and colour changes in a 3 m profile at Remine TSF reveal the thinly layered nature of hydraulically deposited gold tailings, consistent with other gold TSFs (Vermeulen, 2001) and tailings from other commodities (Reid et al., 2022). This PSD variability, often underexplored quantitatively, constitutes a significant deviation from the uniform CC and triaxial specimens that underpin the CPT interpretation methods based on the Been et al. (1986; 1987) framework and which include some of the most widely-used methods in TSFs e.g.(Jefferies et al., 2019; Jung et al., 2025; Plewes et al., 1992; Mozaffari & Ghafghazi, 2024; Shuttle & Cunning, 2007; Shuttle & Jefferies, 1998; Shuttle & Jefferies, 2016; Shuttle et al., 2022).

Furthermore, some of these methods require soil properties such as the slope of the CSL in e-logp' space (λ), dilation properties, plastic parameters, and elastic parameters e.g. (Ayala et al., 2022; Robertson et al., 2019; Shuttle et al., 2022). While PSD may not significantly affect soil properties in some cases (Robertson et al., 2019), it generally affects at least the CSL slope λ and the state-dilatancy property X_{tc} (Jefferies & Been, 2016; Torres-Cruz, 2021). Accordingly, current best practice is to assume that different PSDs yield different properties that have to be determined by laboratory testing (Jefferies & Been, 2016). Characterizing multiple PSDs, as done in the Cadia Valley and Brumadinho investigations (Jefferies et al., 2019; Robertson et al., 2019), is consistent with the presence of varied soils within a single TSF. However, this does not solve the challenge posed by thinly layered deposits in which several soils simultaneously affect the CPT response, making it unclear which soil properties should be used for CPT interpretation. That is, the practicing engineer is left unsure about which tailings gradation should be sent to the laboratory for detailed laboratory testing or if a homogenized sample will yield adequate results. And although ψ variations were not explored herein, it is also possible for ψ to vary across layers, constituting a further deviation from the uniform CC and triaxial specimens.

Thin layering also raises a fundamental question regarding how to validate CPT-based ψ estimates because changes in PSD can affect the height of the CSL in e-logp' space (Thevanayagam et al., 2002; Torres-Cruz, 2019). Accordingly, if an undisturbed layered sample is obtained to confirm a CPT-based ψ estimate, it is not clear which is the CSL that should be used to compare against the overall void ratio of the sample (e.g. Jefferies et al., 2019). Given the

catastrophic consequences of TSF failures, the geotechnical community has to carefully consider how to validate estimates of ψ or of any other engineering-related parameter.

Of the multiple CPT interpretation methods based on the Been et al. (1986; 1987) framework, the "widget" method developed by Shuttle and Cunning (2007), Shuttle and Jefferies (2016), Jefferies et al. (2019), and Shuttle et al. (2022) appears to be the most highly regarded one in the tailings industry. The method is anchored on critical state soil mechanics (CSSM) and was used to investigate the failures at Brumadinho and Cadia Valley (CIMNE, 2021; Jefferies et al., 2019; Robertson et al., 2019). Notwithstanding, a recent comparison between ψ as measured in high-quality samples and ψ as inferred from the widget method concluded that the validation of the method remains unresolved (Fourie et al., 2022). To the authors' knowledge, there is still no evidence that the widget method consistently yields correct ψ values in tailings deposits. It has been suggested that the discrepancy could be due to the fact that the CC testing that underpins the widget method includes predominantly dilatant sands unlike the contractive soils that are of greatest geotechnical interest (Ayala et al., 2022). Our results suggest that thin layering of tailings could also contribute to the discrepancy.

The stark differences between the thin layering of TSFs and the uniform specimens that support the CPT interpretation methods based on Been et al. (1986; 1987) raise questions about the applicability of these methods to TSFs. At the very least, awareness of these differences should lead to caution when interpreting the results of these methods. However, this issue has been largely unaddressed in the literature. It seems possible that the theoretical framework of CSSM coupled with the often-complex nature of the numerical methods used in its implementation may

lead to overestimations of the accuracy of these methods despite the strong mismatch between their assumptions and reality.

Considering the significant laboratory testing effort involved in obtaining precise CSSM parameters of uniform specimens that may only be common in soil laboratories, tailings engineers should consider whether more value could be gained from characterizing high-quality specimens that preserve the in situ thin layering. The latter approach also has limitations because sampling, especially of nonplastic soils, is likely to result in disturbance. Additionally, TSF heterogeneity implies that differences between undisturbed specimens are likely to be larger than differences between reconstituted specimens, making it impossible to precisely characterize a specific "type" of tailings. Notwithstanding, the literature shows that high-quality specimens can play an important role in understanding tailings behaviour. For instance, the investigation of the 1998 Aznalcóllar TSF failure relied on high-quality tailings specimens to characterise strength and deformation properties (Alonso & Gens, 2006). High-quality tailings specimens have also been used in monotonic direct simple shear testing to characterise the peak undrained strength ratio induced by desiccation (Reid et al. 2018b, c). Similarly, an investigation into the Brumadinho TSF failure used high-quality specimens to estimate in situ physical, hydraulic, and geomechanical parameters (da Fonseca et al., 2020).

While it was noted above that several soil properties depend on PSD and are therefore likely to vary within a layered specimen, this is not the case with all properties. For instance, the critical state friction ratio measured under triaxial compression conditions (M_{tc}) remains virtually constant despite strong changes in PSD. This appears to be due to the strong dependence of M_{tc}

on particle shape (Sadrekarimi and Olson, 2011) which in crushed-ore tailings remains highly angular over most particle sizes (Figure 5; Torres-Cruz & Santamarina, 2020; Vermeulen, 2001). We hypothesise that properties that show limited dependence on PSD constitute good candidates to aid the robust characterisation of layered tailings specimens.

5 Conclusions

Current tailings engineering practice emphasises the inference of the state parameter ψ from CPT results which are often supplemented by laboratory testing. The quest for ψ is understandable as it informs whether tailings are contractive or dilative (Been & Jefferies, 1985). However, several widely used CPT interpretation methods are based on CC and triaxial testing of uniform specimens. This raises the question of whether tailings deposits resemble these uniform specimens.

This work documented the layering characteristics of four hydraulically deposited gold TSFs. Ten tube samples that were 25 cm long were extracted from three of the TSFs for laboratory index testing. Additionally, a 3 m deep profile at the fourth TSF was visually appraised for colour changes hypothesised to correspond with changes in PSD or mineralogy. Thin layering, albeit with consistently low plasticity, was observed in all ten tube samples and in the 3 m deep profile, with PSD variability in some samples matching or exceeding the variability observed at entire TSFs. This layered structure, which appears to be common in hydraulically deposited tailings from other commodities (Reid et al., 2022), contrasts starkly with the uniform specimens used in the CC and triaxial testing that underpin several CPT interpretation methods.

The thin layering documented herein is also at odds with a published recommendation to focus CPT interpretation on layers exceeding 0.6 m (Jefferies & Been, 2016). In contrast, the samples and profile examined herein suggest that the thickest uniform layer did not exceed ~0.15 m. These observations raise questions about the fundamental compatibility between CPT interpretation methods based on CC and triaxial results, and thinly layered deposits. This potential incompatibility may be contributing to known limitations in CPT-based ψ estimates, such as those reported for the widget method (Fourie et al., 2022).

Considering that current practice is strongly dominated by the laboratory testing of reconstituted uniform specimens to obtain precise CSSM parameters, our results suggest that there should be more space for the approximate characterisation of specimens that preserve their in situ layered structure. This would be in line with the principle that "it is better to be vaguely right than exactly wrong" (Read, 1920).

6 Acknowledgements

This paper is based on the doctoral research conducted by the first author and supervised by the second one. The authors gratefully acknowledge financial support from Anglo American, and logistic support from DRD Gold, Gold Fields, and Sibanye Stillwater.

7 References

Alonso, E.E., & Gens, A. (2006). Aznalcóllar dam failure. Part 1: Field observations and material properties. Géotechnique, 56(3), 165-183.

ASTM. (2015). ASTM D1587M-15 Standard practice for thin-walled tube sampling of fine-grained soils for geotechnical purposes.

ASTM. (2021). ASTM D7928-21 Standard Test Method for Particle-Size Distribution (Gradation) of Fine-Grained Soils Using the Sedimentation (Hydrometer) Analysis.

Ayala, J., Fourie, A., & Reid, D. (2022). Improved cone penetration test predictions of the state parameter of loose mine tailings. Canadian Geotechnical Journal.

Been, K., & Jefferies, M. (1985). A state parameter for sands. Géotechnique, 35(2), 99-112.

Been, K., & Olivera, R. (2016). Appendix B: Laboratory testing to determine the critical state of sands. In M. Jefferies, & K. Been, Soil Liquefaction - A Critical State Approach. CRC Press.

Been, K., Crooks, J., Becker, D., & Jefferies, M. (1986). The cone penetration test in sands: part I, state parameter interpretation. Géotechnique, 36(2).

Been, K., Jefferies, M., Crooks, J., & Rothenburg, L. (1987). The cone penetration test in sands: part II, general inference of state. Géotechnique, 37(3).

Been, K., Lingnau, B., Crooks, J., & Leach, B. (1987). Cone penetration test calibration for Erksak (Beaufort Sea) sand. Canadian Geotechnical Journal, 24(4).

Blight, G. (2010). Geotechnical Engineering for Mine Waste Storage Facilities. CRC Press.

Boulanger, R., & DeJong, J. (2018). Inverse filtering procedure to correct cone penetration data for thin-layer and transition effects. Cone Penetration Testing 2018. Delft, The Netherlands: CRC Press.

BSI. (1990). BS 1377-2 Methods of test for soils for civil engineering purposes - Classification tests.

Chang, H. (2009). The effect of fabric on the behaviour of gold tailings. PhD Thesis, University of Pretoria.

CIMNE. (2021). Computational analyses of Dam I failure at the Corrego de Feijao mine in Brumadinho.

da Fonseca, A., Cordeiro, D., & Molina-Gómez, F. (2021). Recommended procedures to assess critical state locus from triaxial tests in cohesionless remoulded samples. Geotechnics, 1(1), 95-127.

da Fonseca, A., Cordeiro, D., Molina-Gómez, F., & Fonseca, A. (2020). Annex 1: New site investigation and experimental campaign [IN PORTUGUESE]. In CIMNE, Computational analyses of Dam I failure at the Corrego de Feijao mine in Brumadinho.

Fourie, A., Verdugo, R., Bjelkevik, A., Torres-Cruz, L., & Znidarcic, D. (2022). Geotechnics of mine tailings: a 2022 State of the Art. In Rahman, & Jaksa (Ed.), Proceedings of the 20th ICSMGE-State of the Art and Invited Lectures (pp. 121-183). Sydney, Australia: Australian Geomechanics Society.

Huntsman, S. (1985). Determination of in-situ lateral pressure of cohesionless soils by static cone penetrometer. PhD Thesis. University of California, Berkeley.

Jacobsz, S., & Narainsamy, Y. (2022). Field and laboratory research into the undrained behaviour of tailings at the University of Pretoria. Journal of the Southern African Institute of Mining and Metallurgy, 122(6), 267-273.

Jefferies, M., & Been, K. (2016). Soil Liquefaction - A critical state approach, Second edition. CRC Press.

Jefferies, M., Morgenstern, N., Van Zyl, D., & Wates, J. (2019). Report on NTSF Embankment Failure. Cadia Valley Operations for Ashurst Australia.

Jung, H., Lin, J., & Stark, T. (2025). Sand state parameter from CPT. Canadian Geotechnical Journal, 62, 1-16.

McPhail, G., & Wagner, J. (1987). Disposal of Residues. *In* The extractive metallurgy of gold in South Africa (pp. 655-706).

Morgenstern, N., Vick, S., Viotti, C., & Watts, B. (2016). Report on the Immediate Causes of the Failure of the Fundão Dam.

Mozaffari, M., & Ghafghazi, M. (2024). Material-specific interpretation of the state parameter from drained cone penetration test. Canadian Geotechnical Journal, 61(12), 2858-2872.

Plewes, H., Davies, M., & Jefferies, M. (1992). CPT based screening procedure for evaluating liquefaction susceptibility. Proceedings of the 45th Canadian Geotechnical Conference. Toronto, Canada.

Read, C. (1920). Logic: Deductive and Inductive. London: Simkin, Marshall.

Reid, D., & Fanni, R. (2022). A comparison of intact and reconstituted samples of a silt tailings. Géotechnique, 72(2), 176-188.

Reid, D., Fanni, R., Koh, K., & Orea, I. (2018a). Characterisation of a subaqueously deposited silt iron ore tailings. Géotechnique Letters, 8(4), 278-283.

Reid, D., Fourie, A., & Russell, A. (2018b). Effects of desiccation on shear strength of tailings – comparison of clayey and sandy tailings. Proceedings of Tailings and Mine Waste, 2018.

Reid, D., Fourie, A., Castro, J., & Lupo, J. (2018c). Undrained shear strength evolution with loading on an undisturbed block sample of desiccated gold tailings. Proceedings of Tailings and Mine Waste, 2018.

Reid, D., Fourie, A., & Fanni, R. (2022). Layering – the missing factor in fabric studies? Proceedings of the 20th International Conference on Soil Mechanics and Geotechnical Engineering. Sydney, Australia: Australian Geomechanics Society.

Rezende, V. (2013). Study of the Behavior of a Sand Tailings Dam Constructed Using the Upstream Method [IN PORTUGUESE]. PhD Thesis, Federal University of Ouro Preto.

Robertson, P., de Melo, L., Williams, D., & Wilson, G. (2019). Report of the expert panel on the technical causes of the failure of Feijao Dam I.

Sadrekarimi, A., & Olson S.M. (2011). Critical state friction angle of sands. Géotechnique, 61(9), 771-783.

Shuttle, D., & Cunning, J. (2007). Liquefaction potential of silts from CPTu. Canadian Geotechnical Journal, 44(1), 1-19.

Shuttle, D., & Jefferies, M. (1998). Dimensionless and unbiased CPT interpretation in sand. International Journal for Numerical and Analytical Methods in Geomechanics, 22(5), 351-391.

Shuttle, D., & Jefferies, M. (2016). Determining silt state from CPTu. Geotechnical Research, 3(3), 90-118.

Shuttle, D., Marinelli, F., Brasile, S., & Jefferies, M. (2022). Validation of computational liquefaction for tailings: Tar Island slump. Geotechnical Research, 9(1), 32-55.

Tehrani, F., Arshad, M., Prezzi, M., & Salgado, R. (2017). Physical Modeling of Cone Penetration in Layered Sand. Journal of Geotechnical and Geoenvironmental Engineering, 144(1).

Thevanayagam, S., Shenthan, T., Mohan, S., & Liang, J. (2002). Undrained Fragility of Clean Sands, Silty Sands, and Sandy Silts. Journal of Geotechnical and Geoenvironmental Engineering, 128(10).

Torres-Cruz, L. (2019). Limit void ratios and steady-state line of non-plastic soils. Proceedings of the Institution of Civil Engineers – Geotechnical Engineering, 172(3), 283-295.

Torres-Cruz, L. (2021). The Plewes method: A word of caution. Mining, Metallurgy & Exploration, 38, 1329-1338.

Torres-Cruz, L., & Santamarina, J. (2020). The critical state line of nonplastic tailings. Canadian Geotechnical Journal, 57(10), 1508-1517.

Vermeulen, N. (2001). The composition and state of gold tailings. University of Pretoria, PhD Thesis.

Vick, S. (1990). Planning, Design, and Analysis of Tailings Dams. BiTech Publishers.